Structure and dynamics of liquid $Ni_{36}Zr_{64}$ studied by neutron scattering

D. Holland-Moritz,[1] S. Stüber,[2] H. Hartmann,[1] T. Unruh,[3] T. Hansen,[4] and A. Meyer[1]
[1]*Institut für Materialphysik im Weltraum, Deutsches Zentrum für Luft- und Raumfahrt (DLR), 51170 Köln, Germany*
[2]*Physik Department E13, Technische Universität München, 85747 Garching, Germany*
[3]*Forschungsneutronenquelle Heinz Maier-Leibnitz (FRM II), Technische Universität München, 85747 Garching, Germany*
[4]*Institut Laue-Langevin (ILL), 38042 Grenoble, France*
(Received 24 October 2008; revised manuscript received 21 January 2009; published 23 February 2009)

We report on investigations on the atomic dynamics and the static structure factors of binary $Ni_{36}Zr_{64}$ alloy melts. In order to undercool the melts deeply below the melting temperature and to avoid reactions with crucible materials, the liquids are containerlessly processed by the application of the electromagnetic levitation technique. This technique is combined with quasielastic neutron scattering at the time-of-flight spectrometer TOFTOF of the Munich research reactor (FRM II) and neutron diffraction at the diffractometer D20 of the Institut Laue-Langevin. Partial static structure factors of liquid $Ni_{36}Zr_{64}$ have been derived via isotopic substitution. The quasielastic neutron-scattering experiments indicate a large activation energy for Ni self-diffusion in liquid $Ni_{36}Zr_{64}$ of 0.64 eV. This may result from a peculiar short-range order of the Ni-Zr melts that differs from the icosahedral short-range order that was previously found to prevail in most melts of pure metals and of metallic alloys with a small difference of the atomic radii of the components and that is characterized by a high nearest-neighbor coordination number of $\langle Z \rangle \approx 13.9$, as found by elastic neutron scattering.

DOI: 10.1103/PhysRevB.79.064204 PACS number(s): 61.25.Mv, 66.30.Fq, 61.05.fg

I. INTRODUCTION

Processes on atomic scale determine the physical properties of liquids as well as solidification behavior of melts.[1–3] They are of special importance for understanding the glass formation from the liquid. Here, the nucleation of crystalline phases during cooling of a melt is avoided such that the melt freezes under the formation of an amorphous solid. For glass-forming melts of Ni-P, Pd-Ni-P, and Pd-Ni-Cu-P, it was found that the addition of alloy components to the binary Ni-P system strongly influences the liquidus temperatures and glass-forming ability. Nevertheless, as shown in Fig. 1, it shows a negligible impact on the Ni self-diffusivity.[5,8] For these alloys, the viscosity is coupled with the diffusivity by the Stokes-Einstein relation at elevated temperatures, while deviations from the Stokes-Einstein relation are observed, when decreasing the temperature close to and below the critical temperature T_c of mode-coupling theory. On the other hand, Zr-Ti-Cu-Ni-Be melts forming bulk metallic glasses exhibit considerably smaller values of the Ni self-diffusivity as Pd-(Ni-Cu-)P alloys at similar temperature (Fig. 1) and viscosity and diffusivity are decoupled in the whole temperature regime.[7] Moreover, the activation energies for atomic self-diffusion in the Zr-based melts are significantly larger as compared to those for the self-diffusion in pure Ni (Ref. 6) and Al-Ni alloys.[9,4] Here we address the question of how these differences in the atomic dynamics of the different glass-forming systems originate from peculiarities in the topological and the chemical short-range structure of the different melts.

A careful investigation of the short-range order of alloy melts requires the determination of partial pair-correlation functions: a challenging task prohibitively difficult for multicomponent alloy melts. As will be shown in this work, at a given temperature undercooled binary $Ni_{36}Zr_{64}$ melts exhibit similar Ni self-diffusivities as Zr-Ti-Cu-Ni-Be melts, suggesting similar mechanisms of atomic diffusion in the binary system as in the complex multicomponent alloys. Combined studies on the short-range order and on the atomic dynamics of binary Ni-Zr melts that are presented in this work will help to solve the question for the reason of the differences between the Ni-P-based and the Zr-based glass-forming alloy systems. The possibility of undercooling the Ni-Zr melts will give access to the temperature regime for which diffusivity data on the Zr-Ti-Cu-Ni-Be alloys are available.

In the first part of this work, we present the investigations on the Ni self-diffusion in stable and undercooled $Ni_{36}Zr_{64}$ melts by quasielastic neutron scattering. In the second part, the short-range order of stable $Ni_{36}Zr_{64}$ melts is studied by elastic neutron scattering. In order to determine the full set of partial structure factors of a binary alloy, three different dif-

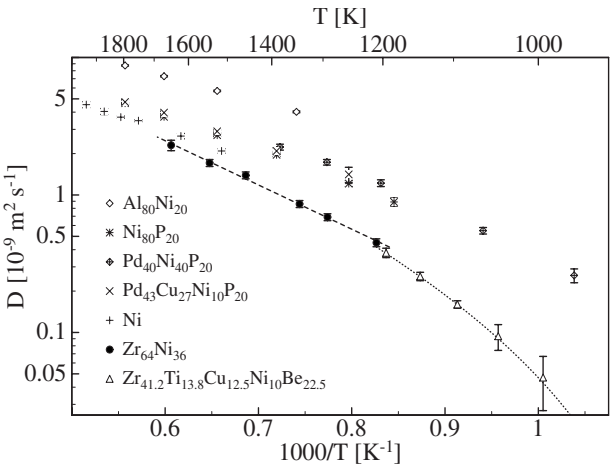

FIG. 1. Temperature dependence of the Ni self-diffusivity in molten $Ni_{36}Zr_{64}$, $Al_{80}Ni_{20}$ (Ref. 4), $Ni_{80}P_{20}$ (Ref. 5), $Pd_{40}Ni_{40}P_{20}$ (Ref. 5), $Pd_{43}Cu_{27}Ni_{10}P_{20}$ (Ref. 5), and Ni (Ref. 6) as well as of the mean Ni and Ti self-diffusivities in liquid $Zr_{41.2}Ti_{13.8}Cu_{12.5}Ni_{10}Be_{22.5}$ (Ref. 7).

fraction experiments with a different scattering contrast of the components are required. In this work, this is achieved by isotopic substitution. We will show that the topological short-range structure of $Ni_{36}Zr_{64}$ melts cannot be described by an icosahedral short-range order that was found to prevail in a large number of melts of pure metals and metallic alloys.[10–13] Moreover, there are indications for a pronounced chemical short-range order in liquid $Ni_{36}Zr_{64}$.

The combined sets of data obtained for liquid $Ni_{36}Zr_{64}$ allow an analysis of the interplay of static structure and atomic diffusion in the framework of mode-coupling theory of the glass transition that is given elsewhere.[14] From the partial static structure factors and mode-coupling theory, the self-diffusion and interdiffusion coefficients for molten $Ni_{36}Zr_{64}$ have been calculated. The absolute value of D_{Ni} from the mode-coupling theory is about two to three times larger than the experimental value, which is within the usual quality of the mode-coupling approximation. The calculations predict that Zr and Ni diffusion proceeds with almost equal rates and thus is more strongly coupled than one would expect for a binary hard-sphere mixture, where only the difference in covalent radii between the two elements is accounted for, but no chemical ordering effects. The experimentally determined partial structure factors, however, give evidence of a pronounced chemical ordering in liquid $Ni_{36}Zr_{64}$. The mode-coupling theory predicts the dynamics of the system using solely this static equilibrium input, establishing a firm relation between the structure and dynamic transport in such melts. The similar self-diffusion coefficients for diffusion of Zr and Ni predicted by the mode-coupling theory are also in contrast with the results of molecular-dynamics simulations of a deeply quenched $Ni_{50}Zr_{50}$ system,[15] where Ni diffusion was found to be significantly faster than Zr diffusion. However, the finding by mode-coupling theory on Ni-Zr qualitatively agrees with recent experimental results for glass-forming Pd-Ni-Cu-P melts, where equal self-diffusion coefficients were observed for Pd and Ni diffusion.[16] These contradicting results motivate further investigations on the interplay of structure and dynamics in Ni-Zr melts.

The mode-coupling theory links the average static structure factor as an input parameter with macroscopic transport coefficients and ensemble averages. In this paper, we will present a detailed discussion of the microscopic structure of the liquid giving rise to this ensemble-averaged structure and its influence on atomic dynamics.

II. EXPERIMENTAL DETAILS

$Ni_{36}Zr_{64}$ samples roughly 1.5 g in mass, which corresponds to a diameter of approximately 7.5 mm, were prepared from the constituents under an Ar atmosphere (purity 99.999 9%) by arc melting. For the determination of the partial static structure factors by isotopic substitution, specimens were alloyed containing ^{60}Ni, ^{58}Ni, and natural Ni.

In order to deeply undercool the liquids below the melting temperature and in order to avoid reactions of the chemically highly reactive Zr-based melts with the sample environment, the liquids are containerlessly processed within a He atmosphere of 99.999 9% purity by employing the electromagnetic levitation technique. A specially designed electromagnetic levitator was used that was utilized already in preceding investigations for neutron-diffraction studies on the short-range order of undercooled metallic melts[17] and that has been modified in order to perform quasielastic neutron-scattering experiments.[6]

The static structure factor of the liquids processed in the electromagnetic levitator was determined by neutron scattering at the high-intensity two-axis diffractometer D20 of the Institut Laue-Langevin (ILL) in Grenoble, France, using a wavelength of the incident neutrons of $\lambda=0.94$ Å. The experimental setup and the data treatment procedure are described in detail in Ref. 17. For the investigation of the dynamics of the liquids, quasielastic neutron-scattering experiments were performed at the time-of-flight spectrometer TOFTOF (Ref. 18) of the Munich research reactor (FRM II) in Garching, Germany, using a wavelength of the incident neutrons of $\lambda=5.1$ Å. The instrumental energy resolution amounts to $\delta E \approx 95$ μeV full width at half maximum (FWHM) at zero energy transfer. It has been verified that even for strongly incoherent-scattering samples such as those of pure Ni, the precise determination of diffusion coefficients is not hampered by the influences of multiple scattering despite of the sample geometry (diameter is approximately 7.5 mm).[6]

III. RESULTS AND DISCUSSION

A. Atomic dynamics of liquid Zr-Ni

Quasielastic neutron-scattering experiments were performed for liquid $Ni_{36}Zr_{64}$ at different temperatures ranging from temperatures above the liquidus temperature T_L down to temperatures in the metastable regime of an undercooled melt below T_L. As an example, the upper part of Fig. 2 shows the quasielastic range of the scattering law $S(Q,\omega)$ for undercooled $Ni_{36}Zr_{64}$ at $T=1210$ K ($T_L=1283$ K) at two different wave vectors ($Q=0.8$ Å^{-1} and $Q=1.8$ Å^{-1}); whereas in the lower part of Fig. 2 $S(Q,\omega)$ is depicted for two different temperatures ($T=1290$ K and $T=1650$ K) at a wave vector of $Q=0.9$ Å^{-1}. The quasielastic signal can be well described with a Lorentzian function convoluted with the instrumental energy resolution function measured at 290 K vanadium (lines in Fig. 2). It can be clearly seen that the full width at half maximum Γ of the Lorentzian function at contant Q decreases with decreasing temperature. Moreover, at constant temperature Γ rises if Q is increased. Γ is shown in Fig. 3 for different temperatures as a function of Q^2.

For small momentum transfer (below $Q \approx 1.2$ Å^{-1}), the measured signal is dominated by the incoherent scattering of the Ni atoms [incoherent-scattering cross sections: $\sigma_{inc}(^{nat}Ni)=5.2$ b and $\sigma_{inc}(Zr)=0.02$ b] and the mean Ni self-diffusivity is related with Γ by $D=\Gamma Q^{-2}/2\hbar$.[19,20] Hence, at small Q, the slope of the $\Gamma(Q^2)$ curves (Fig. 3) gives the Ni self-diffusivity.

The Ni self-diffusivities determined for $Ni_{36}Zr_{64}$ melts as a function of temperature are compiled in Table I and are plotted in Fig. 1. Also shown in Fig. 1 are the results from former measurements of the Ni self-diffusivity in pure Ni,[6]

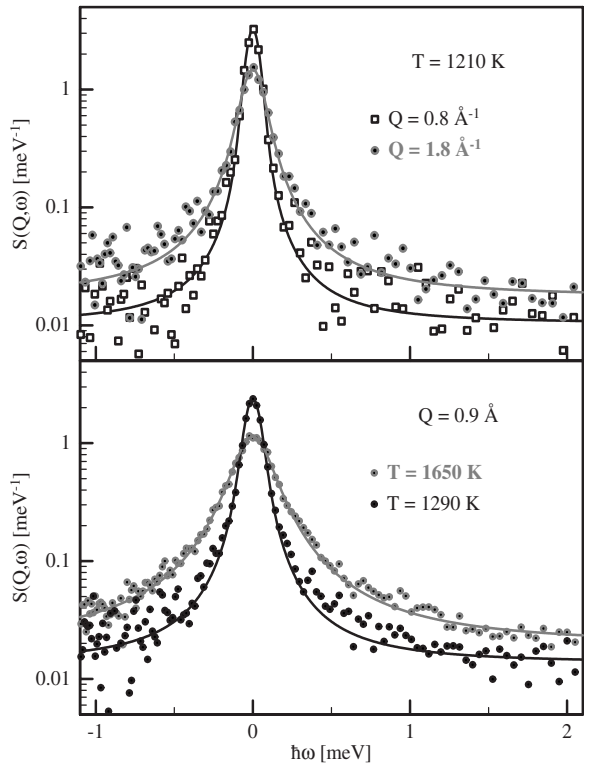

FIG. 2. Scattering law for liquid $Ni_{36}Zr_{64}$ at $T=1210$ K for two different wave vectors $Q=0.8$ Å^{-1} and $Q=1.8$ Å^{-1} (upper part) and at $Q=0.9$ Å^{-1} for two different temperatures $T=1290$ K and $T=1650$ K (lower part).

$Al_{80}Ni_{20}$,[4] $Ni_{80}P_{20}$,[5] $Pd_{40}Ni_{40}P_{20}$,[5] and $Pd_{43}Cu_{27}Ni_{10}P_{20}$,[5] and of the mean Ni and Ti self-diffusivity in melts of glass-forming $Zr_{41.2}Ti_{13.8}Cu_{12.5}Ni_{10}Be_{22.5}$.[7] At a given temperature, the absolute values of the Ni self-diffusion coefficients measured for $Ni_{36}Zr_{64}$ are considerably smaller than those found for Ni, Al-Ni, and Ni-(Pd-Cu-)P, while the slope of the $D(T)$ curve is higher. However, the diffusivity values of the binary $Ni_{36}Zr_{64}$ melts extend the $D(T)$ curve determined for $Zr_{41.2}Ti_{13.8}Cu_{12.5}Ni_{10}Be_{22.5}$ to higher temperatures. At temperatures around 1200 K, even the slopes of the curves differ only slightly despite of the different alloy compositions. This indicates that the addition of the other alloy components (Ti, Cu, and Be) to the binary Ni-Zr alloy has only a small influence on the Ni self-diffusivity. A similar behavior has also been observed for the Ni-(Pd-Cu-)P system, where the addition of Pd and Cu to the binary Ni-P alloy has only a minor impact on the Ni self-diffusion (see also Fig. 1).[5]

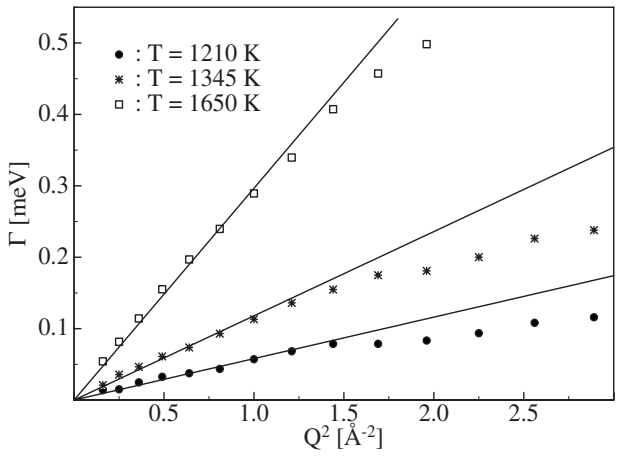

FIG. 3. Full width at half maximum Γ of the Lorentzian curves as a function of Q^2 for liquid $Ni_{36}Zr_{64}$ at three different temperatures. The errors are smaller than the symbol size.

TABLE I. Ni self-diffusion coefficients of $Ni_{36}Zr_{64}$ melts determined by quasielastic neutron scattering ($T_L=1283$ K).

T (K)	D [10^{-9} m^2/s]
1210 ± 5	0.45 ± 0.06
1290 ± 5	0.70 ± 0.06
1345 ± 5	0.90 ± 0.06
1455 ± 5	1.4 ± 0.1
1545 ± 5	1.7 ± 0.1
1650 ± 5	2.3 ± 0.2

The $D(T)$ of liquid $Ni_{36}Zr_{64}$ shows essentially an Arrhenius-type behavior $D=D_0\exp(-E_A/k_BT)$ in the investigated temperature regimes with $E_A=0.64\pm0.02$ eV and $D_0=(2.1\pm0.3)\times10^{-7}$ m^2/s (dashed line in Fig. 1). These activation energies for Ni self-diffusion are large as compared to the values observed in other melts. For instance, our former investigations on pure Ni gave $E_A(\mathrm{Ni})=0.47$ eV.[6] For liquid $Al_{80}Ni_{20}$, a value of $E_A(\mathrm{Al\text{-}Ni})=0.36$ eV is reported.[4] Even a lower activation energy of $E_A(\mathrm{Si\text{-}Ni})=0.28$ eV has been determined for the Ni self-diffusion in Si-rich Si-Ni melts.[21] The temperature range in which an Arrhenius-type behavior of the self-diffusion coefficient has been observed is considerably above the critical temperature T_c of mode-coupling theory. When approaching T_c, mode-coupling theory predicts a $(T\text{-}T_c)^\gamma$ dependence of the diffusivity. Indeed, as reported earlier,[7] the temperature dependence of the mean Ni and Ti self-diffusivity in liquid $Zr_{41.2}Ti_{13.8}Cu_{12.5}Ni_{10}Be_{22.5}$ is well described by a $(T\text{-}T_c)^\gamma$ law with $T_c=850$ K and $\gamma=2.5$ (dotted line in Fig. 1).

B. Short-range order of liquid $Ni_{36}Zr_{64}$

In order to find the reasons for the peculiar atomic dynamics in the Ni-Zr-based melts, we have investigated the short-range structure of three $Ni_{36}Zr_{64}$ melts prepared with natural Ni, ^{58}Ni, and ^{60}Ni at a temperature of $T=1375$ K by elastic neutron scattering. Figure 4 shows the resulting three total static structure factors $S(Q)$. Marked differences between these structure factors are visible. The strong dependence of the shape of the total structure factors on the scattering cross sections of the alloy components highlights that the analysis of the short-range order in these alloy melts is not possible using one total structure factor from one diffraction experiment only, but it is necessary to determine the full set of partial structure factors. We have calculated the partial structure factors from the three total structure factors within the Faber-Ziman[22] and the Bhatia-Thornton formalism.[23]

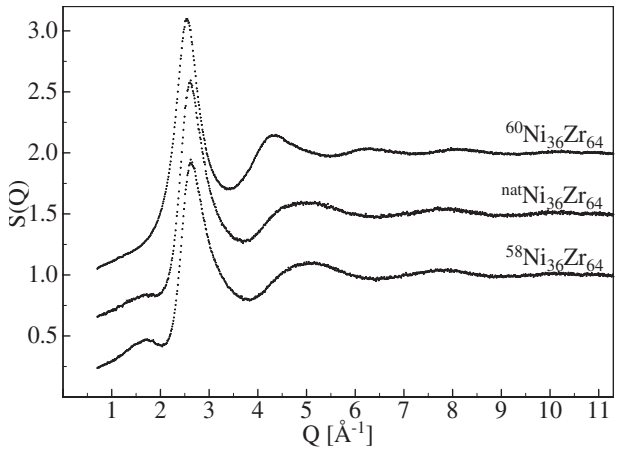

FIG. 4. Total structure factors measured by neutron scattering for $^{58}Ni_{36}Zr_{64}$, $^{60}Ni_{36}Zr_{64}$, and $^{nat}Ni_{36}Zr_{64}$ at $T=1375$ K. The curves are shifted by multiples of 0.5 along the vertical axis.

The static Faber-Ziman structure factors $S_{ZrZr}(Q)$, $S_{NiZr}(Q)$, and $S_{NiNi}(Q)$ describe the contributions to $S(Q)$, which result from the three different types of atomic pairs (Zr-Zr, Ni-Zr, and Ni-Ni). Within the Bhatia-Thornton formalism, the static partial structure factor $S_{NN}(Q)$ describes solely the topological short-range order of the system, $S_{CC}(Q)$ the chemical short-range order, and $S_{NC}(Q)$ the correlation of number density and chemical composition. The upper part of Fig. 5 shows the Bhatia Thornton structure factors and the lower part the Faber-Ziman structure factors determined from the neutron-scattering experiments for liquid $Ni_{36}Zr_{64}$ at $T=1375$ K. The corresponding pair-correlation functions $g_{NN}(r)$, $g_{CC}(r)$, $g_{NC}(r)$, $g_{ZrZr}(r)$, $g_{NiNi}(r)$, and $g_{NiZr}(r)$ calculated by Fourier transformation from the static structure factors are depicted in Fig. 6. The cutoff of the integration has been $Q_{max}=11$ Å^{-1} and no damping has been applied to $S(Q)$-1. Some small oscillations visible in the pair-correlation functions are artifacts resulting from the limited Q range available for Fourier transformation.

The Bhatia-Thornton pair-correlation function g_{CC} is characterized by a remarkable minimum at $r\approx 2.7$ Å. This minimum is a signature of a chemical short-range order prevailing in the liquid, which results in an affinity for the formation of Ni-Zr nearest neighbors. The same conclusion can be drawn from the fact that the first maximum of the Faber-Ziman pair-correlation function $g_{NiZr}(r)$ is significantly larger than the first maxima of $g_{NiNi}(r)$ and $g_{ZrZr}(r)$.

From the first maxima of $g_{NN}(r)$, $g_{NiNi}(r)$, $g_{ZrZr}(r)$, and $g_{NiZr}(r)$, the corresponding nearest-neighbor distances are determined for the different types of neighbors that are compiled in Table II. Moreover, the different nearest-neighbor coordination numbers Z_{ij} $(i,j=\mathrm{N,Zr,Ni})$ are calculated by integrating the partial radial distribution function $4\pi c_j \rho r^2 g_{ij}(r)$ over its first maximum (with the first and second minimum as integration boundaries). c_j denotes the composition of component j and ρ denotes the atomic density. A value of $\rho=0.052$ at./Å^3 is used that is inferred from the measurements of the density of $Ni_{36}Zr_{64}$ melts employing electromagnetic levitation. There are other methods to determine Z_{ij},[26] which may lead to a spread of the absolute values

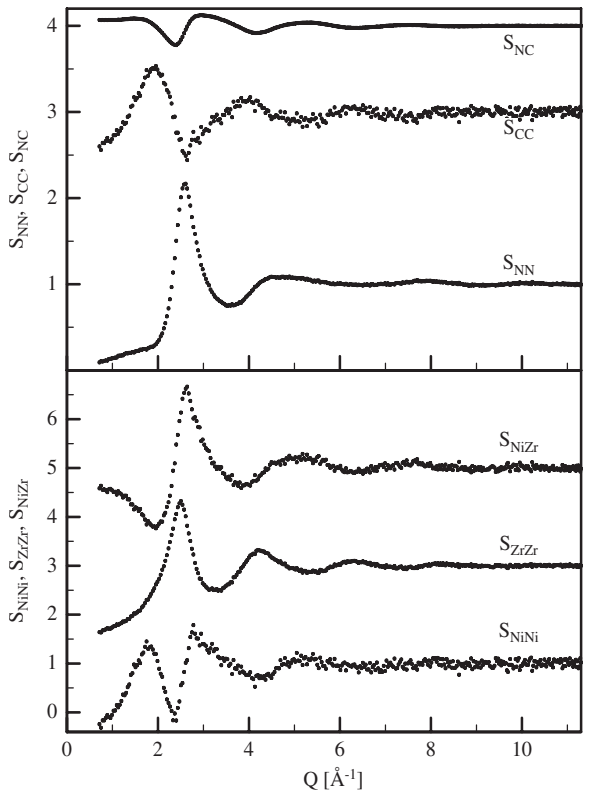

FIG. 5. Static partial Bhatia-Thornton (upper part) and Faber-Ziman (lower part) structure factors of liquid $Ni_{36}Zr_{64}$ at $T=1375$ K. The curves for S_{ZrZr} and S_{CC} are shifted by two and S_{NC} and S_{NiZr} are shifted by four along the vertical axis.

of Z_{ij} by about 10% (not included in the errors of Table II). The nearest-neighbor coordination number Z_{NN} inferred from the Bhatia-Thornton pair-correlation function g_{NN} describes the average number of nearest neighbors of an arbitrary atom without distinguishing the different elements. The coordination numbers Z_{ij} $(i,j=\mathrm{Zr,Ni})$ calculated from the Faber-Ziman pair-correlation functions describe the number of neighbors of type i around a j atom. The average coordination number $\langle Z\rangle = c_i(Z_{ii}+Z_{ji})+c_j(Z_{jj}+Z_{ij})$ determined from the Faber-Ziman partial coordination numbers is in agreement with Z_{NN} that is calculated from the Bhatia-Thornton pair-correlation function g_{NN}. In Table II the nearest-neighbor distances and the coordination numbers we inferred for liquid $Ni_{36}Zr_{64}$ are compared with the corresponding values reported in literature for liquids of the pure elements Ni (Ref. 10) and Zr,[10] for amorphous $Ni_{25}Zr_{75}$,[24] and for $Al_{80}Ni_{20}$ (Ref. 25) and $Al_{13}(Co,Fe)_4$ (Ref. 12) melts. The values we determined for liquid $Ni_{36}Zr_{64}$ are close to the literature values for amorphous $Ni_{25}Zr_{75}$. The larger Z_{NiNi} and Z_{NiZr} observed for $Ni_{36}Zr_{64}$ may be explained by the higher Ni concentration of this alloy. The Ni-Ni and Zr-Zr nearest-neighbor distances found in $Ni_{36}Zr_{64}$ are slightly larger than in the molten pure elements, while the Ni-Zr distance is slightly smaller than the average of the nearest-neighbor distances of both pure elements. The average coordination number $\langle Z\rangle \approx 13.9$ measured for liquid $Ni_{36}Zr_{64}$ is considerably higher than the typical values of $\langle Z\rangle \approx 12$ reported for most metallic melts,[10,26] including the melts of the

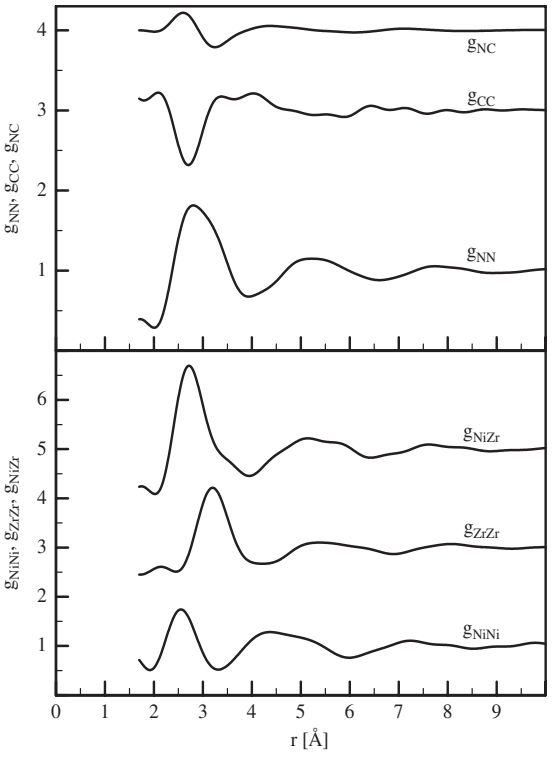

FIG. 6. Partial Bhatia-Thornton (upper part) and Faber-Ziman (lower part) pair-correlation functions of liquid $Ni_{36}Zr_{64}$ at $T=1375$ K. The curves for g_{ZrZr} and g_{CC} are shifted by two, g_{NC} is shifted by three, and g_{NiZr} is shifted by four along the vertical axis.

pure components Ni and Zr and Al-transition metal (TM) alloys as compiled in Table II. This indicates a comparatively high local density of packing in molten $Ni_{36}Zr_{64}$.

For a further analysis of the topological short-range order of liquid $Ni_{36}Zr_{64}$, $S_{NN}(Q)$ was modeled in the regime of large Q vectors by assuming that the short-range order is dominated by one type of structural units. The used simulation method[27,28] has the advantage that it depends on three free parameters only. These are the shortest mean distance of atoms $\langle r_0 \rangle$ within the unit, its mean thermal variation $\langle \delta r_0^2 \rangle$ that determines the Debye-Waller factor $\exp(-2Q^2 < \delta r_0^2 > /3)$, and the concentration X of atoms belonging to the aggregates that make up the short-range order in the liquid.

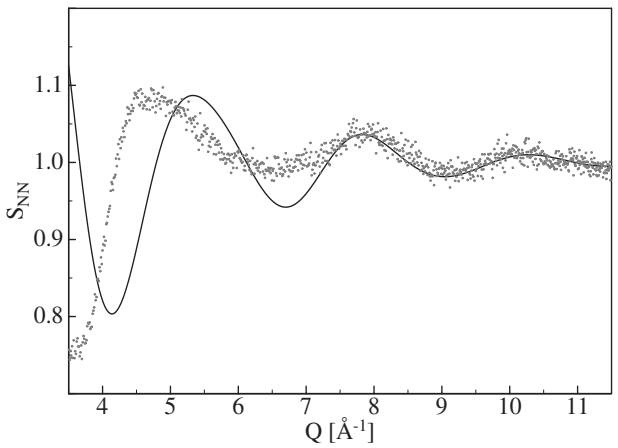

FIG. 7. Measured (gray symbols) and simulated (solid line) S_{NN} of liquid $Ni_{36}Zr_{64}$ at large momentum transfer. For the simulation, an icosahedral short-range order is assumed to prevail in the melt.

The parameters are adjusted such that the best fit of the experimentally determined $S_{NN}(Q)$ is obtained especially at large Q vectors. This regime of large Q vectors is mainly determined by the short-range order because the contributions from the less tightly bound intercluster distances are damped out by thermal motions. Effects of long-range correlations which affect $S_{NN}(Q)$ mainly at small Q vectors are neglected in this simple approach. As an example, the result of a simulation under an assumption of an icosahedral short-range order that has been frequently reported to prevail in metallic melts (see discussion below) is shown in Fig. 7 together with the experimentally determined $S_{NN}(Q)$ at large momentum transfer. No reasonable description of the measured structure factor is obtained for icosahedral short-range order. Also for a dodecahedral, fcc, hcp, or bcc type of short-range order, the simulated structure factors disagree with the experimental data. Obviously a more complex type of short-range order prevails in liquid $Ni_{36}Zr_{64}$.

We also modeled the structure factors under an assumption of a trigonal prismatic short-range order as suggested by molecular-dynamics investigations for amorphous Zr-Ni-Al alloys.[29] For this type of short-range order, a good description of the measured structure factor was only obtained if atomic distances were assumed that are in contradiction with

TABLE II. Nearest-neighbor distances and coordination numbers inferred from the partial pair-correlation functions for the different types of neighbors. In case data has been measured as function of temperature, the range of variation in the values with increasing temperature is given.

	T (K)	r_{NN} (Å)	Z_{NN}	r_{NiNi} (Å)	Z_{NiNi} (Z_{TMTM})	r_{ZrZr} (Å)	Z_{ZrZr} (Z_{AlAl})	r_{NiZr} (Å)	Z_{ZrNi} (Z_{AlTM})	Z_{NiZr} (Z_{TMAl})	$\langle Z \rangle$	Ref.
$Ni_{36}Zr_{64}$	1375	2.80 ± 0.02	13.8 ± 0.5	2.55 ± 0.02	2.5 ± 0.5	3.20 ± 0.02	10.4 ± 0.5	2.69 ± 0.02	8.8 ± 0.5	5.0 ± 0.5	13.9 ± 0.5	This work
Ni	1435–1905	2.49–2.48	12.3–11.2	2.49–2.48	12.3–11.2						12.3–11.2	10
Zr	1830–2290	3.13–3.12	12.2–11.9			3.13–3.12	12.2–11.9				12.2–11.9	10
$Ni_{25}Zr_{75}$ (amorphous)				2.63	1.8	3.16	10.9	2.66	8.6	2.8	12.9	24
$Al_{80}Ni_{20}$				2.63	1.65		9.6		10.9	2.7	12.6	25
$Al_{13}(Co,Fe)_4$	T_L+30 K		12.3		1.9		9.8		9.7	3.0	12.5	12

the nearest-neighbor distances inferred from the diffraction studies (Table II) such as a Ni-Zr distance of approximately 3.2 Å.

Preceding investigations on the short-range order of monatomic metallic melts provided strong evidence that an icosahedral or, more generally, a polytetrahedral short-range order prevails in the liquid phase from theoretical modeling[30–32] as well as from experimental[10,11,13,33,34] studies. Diffraction experiments[10,11,13,33,34] have proven that in general this short-range order of the liquid phase is independent of the structure of the corresponding solid phase that is formed from the liquid during solidification. The icosahedral short-range order has already been observed for stable melts above the melting point and it becomes more pronounced if the liquids are undercooled below the melting temperature. There are indications that this short-range order consists of larger polytetrahedral units such as dodecahedra.[10]

As shown before, for $Ni_{36}Zr_{64}$ the assumption of an icosahedral topological short-range order in the melt is not able to describe the measured S_{NN}. Also the high nearest-neighbor coordination numbers Z_{NN} are not in agreement with the icosahedral short-range order, which suggest $Z_{NN} \sim 12$. It is important to note that the above-mentioned investigations in which an icosahedral short-range order was found are concerned with monatomic metallic melts. For alloy melts, such as $Ni_{36}Zr_{64}$, however, the situation is more complex. While for monatomic systems an icosahedron is characterized by high density of packing, for alloys with a large difference in the atomic radii the formation of units with a different symmetry may be favorable. As long as the atomic radii of the alloy components are similar, it can be assumed that again an icosahedral short-range order will be advantageous. Jónsson and Andersen,[35] for instance, investigated a binary Lennard-Jones liquid, which contained 20% of *A* atoms that were 25% larger than the *B* atoms by molecular-dynamics simulations. In the deeply undercooled liquid, 61% of all atoms were within an icosahedral environment.

On the other hand, molecular-dynamics calculations by Dasgupta *et al.*[36] on a binary Lennard-Jones liquid consisting of an equal number of atoms—but with one species having a 1.6 times larger radius than the other—exhibited no indication for the development of an icosahedral short-range order in the undercooled melt.

Ronchetti and Cozzini[37] suggested that these contradicting findings may be a result of the difference in the atomic radii and the composition of the simulated binary systems. They studied the structure of 13-atom clusters in a binary Lennard-Jones liquid consisting of large *A* atoms (radius R_A) and smaller *B* atoms (radius R_B) as a function of the ratio R_A/R_B and of the concentration c_B of *B* atoms. For $R_A/R_B = 1.25$, icosahedral units are dominant in the composition ranges $c_B < 4/13 \approx 30$ at % and $c_B > 8/13 \approx 62$ at %; while at compositions around 50 at. % no favored structure was observed. With an increasing ratio R_A/R_B the composition ranges, in which icosahedral units are dominant, shrink. For $R_A/R_B = 1.6$ icosahedral symmetry is only preferred for $c_B < 1/13 \approx 7.7$ at % and $c_B > 69$ at %. In a composition interval of $1/13 \approx 7.7$ at %, $< c_B < 5/13 \approx 38$ at % clusters consisting of 10 atoms are preferred, while in the remaining range no dominant structure was found.

The molecular-dynamics studies of Jónsson and Andersen,[35] which found an icosahedral short-range order, were performed for systems, which have a composition ($c_B < 30$ at %) and a R_A/R_B ratio (R_A/R_B ratio ≤ 1.25) at which icosahedral clusters should be favorable according to the calculations by Ronchetti and Cozzini.[37] Also the results from Dasgupta *et al.*[36] are consistent with the suggestions by Ronchetti and Cozzini[37] because for the parameters $R_A/R_B = 1.6$ and $c_B = 50$ at %, icosahedral clusters are predicted to be disadvantageous.

From the experimental side, the short-range order of a large variety of alloy melts has been investigated by diffraction techniques. The investigated systems include Al-based melts forming quasicrystalline or polytetrahedral solid phases [Al-(Pd-)Mn,[27,28] $Al_{13}(Co,Fe)_4$,[12] and $Al_{60}Cu_{34}Fe_6$ (Ref. 38)]; $Co_{75}Pd_{25}$ melts[39] that form crystals with an fcc structure and $Ti_{72.3}Fe_{27.7}$ (Ref. 40) liquids, which form β (Ti,Fe) (bcc structure) as the primary phase during solidification. The studies give a direct experimental proof of an icosahedral short-range order prevailing in all of these alloy melts. As for melts of pure metals, this icosahedral short-range order in the liquid phase is already observed at temperatures above the melting point and becomes more pronounced if the temperature of the melt is decreased. For the Al-based systems and for $Ti_{72.3}Fe_{27.7}$, the icosahedral topological order is accompanied by a pronounced chemical order such that Al-TM or Ti-Fe nearest neighbors are preferred.[12,27,28,40] All of these alloys are characterized by a moderate difference of the atomic radii of the components with ratios of the atomic radii smaller than 1.25. For binary alloys, at such R_A/R_B ratios the molecular-dynamics calculations of Ronchetti and Cozzini[37] predict an icosahedral short-range order in wide composition ranges, which is consistent with the experimental findings. Please note that for the ternary Al-based alloys discussed before, the difference of the atomic radii of the TM atoms is very small such that these alloys can also be considered as binary Al-TM alloys, if only the atomic radii are concerned.

Ni-Zr alloys, however, exhibit a significantly larger difference of the atomic radii of the components than the binary alloys for which an icosahedral short-range order was found (Goldschmidt radii: $R_{Zr} = 1.60$ Å, $R_{Ni} = 1.24$ Å, and $R_{Zr}/R_{Ni} = 1.29$). As suggested by the molecular-dynamics calculations,[36,37] this may promote the formation of alternative structures different from the icosahedral one.

We have shown in Sec. III A that the activation energies for the Ni self-diffusion in the Ni-Zr liquids are significantly higher than the values determined for liquid Ni and $Al_{80}Ni_{20}$. The absolute values of the Ni self-diffusion coefficients in Ni-Zr are more than 1 order of magnitude smaller than those in $Al_{80}Ni_{20}$. For pure Ni, the static structure factors measured by neutron scattering[10] and diffraction of synchrotron radiation[11] are indicative of an icosahedral short-range order in the melt.[10,11] For $Al_{80}Ni_{20}$, partial structure factors were calculated by molecular-dynamics simulations.[4,41] The simulations are indicative of a chemical short-range order such that Al-Ni nearest neighbors are preferred. The Bhatia-Thornton structure factor S_{NN} calculated for liquid $Al_{80}Ni_{20}$ develops a shoulder on the second maximum if the temperature is decreased. Such a shoulder is considered as a first

indication of an icosahedral short-range order prevailing in the melt.[1] Our diffraction studies have revealed that for $Ni_{36}Zr_{64}$, similar as predicted for $Al_{80}Ni_{20}$, there is a chemical short-range order such that heterogeneous nearest neighbors are preferred. The topological short-range order of $Ni_{36}Zr_{64}$ melts, however, is different from an icosahedral one. It may be speculated if the marked differences in the activation energies for Ni self-diffusion observed between liquid Ni-Zr on one side and Ni and $Al_{80}Ni_{20}$ on the other side are a result of the different topological short-range order. Especially, the comparatively large average coordination number $\langle Z \rangle \approx 13.9$ observed for $Ni_{36}Zr_{64}$ melts suggests a large local density of packing. This may result to the observed large activation energy for atomic diffusion.

The experimental observation or theoretical prediction of icosahedral short-range order in a large number of metallic melts, including some glass-forming systems, resulted in speculations about a possible link between glass-forming ability and icosahedral short-range order.[42] This idea has been supported by the observation that some glass-forming melts form metastable quasicrystalline phases as primary phases during devitrification.[43] In this work, however, we provide evidence that the short-range order in glass-forming $Ni_{36}Zr_{64}$ melts, which is the binary basis system of many multicomponent Zr-based glass-forming alloys, is not dominated by icosahedral aggregates. From this we conclude that the glass-forming ability is not tied to a special kind of short-range order in the melts but depends on more general factors such as a high density of packing combined with rather small atomic diffusion coefficients or structural frustration (many competing solid structures). As discussed before, icosahedral short-range order is predicted to be the favorable structure especially for melts with a small difference of the atomic radii of the components. A great variety of glass-forming alloy systems, however, is characterized by large differences of their atomic radii. In such case, alternative types of short-range order may allow for a higher density of packing than the icosahedral one and consequently these types of short-range order may be preferred.[44]

IV. CONCLUSIONS

We have determined partial structure factors of liquid $Ni_{36}Zr_{64}$ by neutron scattering using the technique of isotopic substitution. The $Ni_{36}Zr_{64}$ melts exhibit a pronounced chemical short-range order such that the Ni-Zr nearest neighbors are preferred. Different from most other metallic melts investigated so far, we found no indications for the existence of an icosahedral short-range order in stable $Ni_{36}Zr_{64}$ melts. This may result from the comparatively larger difference of the atomic radii of Ni and Zr ($R_{Zr}/R_{Ni}=1.29$).

The atomic dynamics of stable and undercooled $Ni_{36}Zr_{64}$ melts was studied by quasielastic neutron scattering. In the investigated temperature regime, the temperature dependence of the diffusion coefficients can be reasonably well described by an Arrhenius behavior. The $D(T)$ values determined for $Ni_{36}Zr_{64}$ are on the same curve as those reported for glass-forming Zr-Ti-Ni-Cu-Be alloys. This may suggest that for these systems, Ni self-diffusion is governed by similar microscopic processes.

The activation energy for Ni self-diffusion is significantly larger for liquid Ni-Zr than for pure Ni and $Al_{80}Ni_{20}$ and the absolute values of the Ni self-diffusion coefficients in the range of $0.45-2.3\times10^{-9}$ m^2/s are more than 1 order of magnitude smaller than the diffusivities reported for liquid $Al_{80}Ni_{20}$. This might be a result of the different topological short-range order in these systems.

ACKNOWLEDGMENTS

The authors thank O. Heinen, D. M. Herlach, J. Horbach, D. Menke, Th. Voigtmann, and F. Yang for fruitful discussions and/or support during the preparation and performance of the experiments. We thank J. Brillo for providing the density measurements. Financial support by the Deutsche Forschungsgemeinschaft (DFG) within the priority program 1120 under Contracts No. Ho1942/4-1 and No. Me1958/2-3 is gratefully acknowledged.

[1] D. R. Nelson and F. Spaepen, in *Solid State Phys*, edited by H. Ehrenreich, F. Seitz, and D. Turnbull (Academic, New York, 1989), Vol. 42, p. 1.
[2] D. Holland-Moritz, Int. J. Non-Equilib. Process. **11**, 169 (1998).
[3] D. M. Herlach, P. Galenko, and D. Holland-Moritz, in *Metastable Solids from Undercooled Melts*, Pergamon Materials Series, edited by R. W. Cahn (Elsevier, Oxford, 2007).
[4] J. Horbach, S. K. Das, A. Griesche, M.-P. Macht, G. Frohberg, and A. Meyer, Phys. Rev. B **75**, 174304 (2007).
[5] S. Mavila Chathoth, A. Meyer, M. M. Koza, and F. Juranyi, Appl. Phys. Lett. **85**, 4881 (2004).
[6] A. Meyer, S. Stüber, D. Holland-Moritz, O. Heinen, and T. Unruh, Phys. Rev. B **77**, 092201 (2008).
[7] A. Meyer, W. Petry, M. Koza, and M.-P. Macht, Appl. Phys. Lett. **83**, 3894 (2003).
[8] A. Meyer, Phys. Rev. B **66**, 134205 (2002).
[9] S. K. Das, J. Horbach, M. M. Koza, S. Mavila Chathoth, and A. Meyer, Appl. Phys. Lett. **86**, 011918 (2005).
[10] T. Schenk, D. Holland-Moritz, V. Simonet, R. Bellissent, and D. M. Herlach, Phys. Rev. Lett. **89**, 075507 (2002).
[11] G. W. Lee, A. K. Gangopadhyay, K. F. Kelton, R. W. Hyers, T. J. Rathz, J. R. Rogers, and D. S. Robinson, Phys. Rev. Lett. **93**, 037802 (2004).
[12] T. Schenk, V. Simonet, D. Holland-Moritz, R. Bellissent, T. Hansen, P. Convert, and D. M. Herlach, Europhys. Lett. **65**, 34 (2004).
[13] K. F. Kelton, A. L. Greer, D. M. Herlach, and D. Holland-Moritz, MRS Bull. **29**, 940 (2004).
[14] T. Voigtmann, A. Meyer, D. Holland-Moritz, S. Stüber, T. Hansen, and T. Unruh, Europhys. Lett. **82**, 66001 (2008).
[15] H. Teichler, J. Non-Cryst. Solids **293-295**, 339 (2001).
[16] A. Griesche, M. P. Macht, S. Suzuki, K.-H. Kraatz, and G. Froh-

berg, Scr. Mater. **57**, 477 (2007).
[17] D. Holland-Moritz, T. Schenk, P. Convert, T. Hansen, and D. M. Herlach, Meas. Sci. Technol. **16**, 372 (2005).
[18] T. Unruh, J. Neuhaus, and W. Petry, Nucl. Instrum. Methods Phys. Res. A **580**, 1414 (2007).
[19] J. P. Hansen and I. R. McDonald, *Theory of Simple Liquids* (Academic, London, 1976).
[20] J. P. Boon and S. Yip, *Molecular Hydrodynamics* (McGraw-Hill, New York, 1980).
[21] A. I. Pommrich, A. Meyer, D. Holland-Moritz, and T. Unruh, Appl. Phys. Lett. **92**, 241922 (2008).
[22] T. E. Faber and J. M. Ziman, Philos. Mag. **11**, 153 (1965).
[23] A. B. Bhatia and D. E. Thornton, Phys. Rev. B **2**, 3004 (1970).
[24] W.-M. Kuschke, P. Lamparter, and S. Steeb, Z. Naturforsch., A: Phys. Sci. **46a**, 951 (1991).
[25] M. Maret, T. Pomme, A. Pasturel, and P. Chieux, Phys. Rev. B **42**, 1598 (1990).
[26] Y. Waseda, *The Structure of Non-Crystalline Materials* (McGraw-Hill, New York, 1980).
[27] V. Simonet, F. Hippert, H. Klein, M. Audier, R. Bellissent, H. Fischer, A. P. Murani, and D. Boursier, Phys. Rev. B **58**, 6273 (1998).
[28] V. Simonet, F. Hippert, M. Audier, and R. Bellissent, Phys. Rev. B **65**, 024203 (2001).
[29] M. Guerdane and H. Teichler, Phys. Rev. B **65**, 014203 (2001).
[30] F. C. Frank, Proc. R. Soc. London, Ser. A **215**, 43 (1952).
[31] P. J. Steinhardt, D. R. Nelson, and M. Ronchetti, Phys. Rev. B **28**, 784 (1983).
[32] S. Nosé and F. Yonezawa, Solid State Commun. **56**, 1005 (1985).
[33] D. Holland-Moritz, T. Schenk, R. Bellissent, V. Simonet, F. Funakoshi, J. M. Merino, T. Buslaps, and S. Reutzel, J. Non-Cryst. Solids **312-314**, 47 (2002).
[34] D. Holland-Moritz, O. Heinen, R. Bellissent, and T. Schenk, Mater. Sci. Eng., A **449-451**, 42 (2007).
[35] H. Jónsson and H. C. Andersen, Phys. Rev. Lett. **60**, 2295 (1988).
[36] C. Dasgupta, A. V. Indrani, S. Ramaswamy, and M. K. Phani, Europhys. Lett. **15**, 307 (1991).
[37] M. Ronchetti and S. Cozzini, Mater. Sci. Eng., A **178**, 19 (1994).
[38] D. Holland-Moritz, T. Schenk, V. Simonet, and R. Bellissent, Philos. Mag. **86**, 255 (2006).
[39] D. Holland-Moritz, T. Schenk, V. Simonet, R. Bellissent, and D. M. Herlach, J. Metastable Nanocryst. Mater. **24-25**, 305 (2005).
[40] D. Holland-Moritz, O. Heinen, R. Bellissent, T. Schenk, and D. M. Herlach, Int. J. Mater. Res. **97**, 948 (2006).
[41] S. K. Das, J. Horbach, and Th. Voigtmann, Phys. Rev. B **78**, 064208 (2008).
[42] H. Tanaka, J. Phys.: Condens. Matter **15**, L491 (2003).
[43] U. Köster, J. Meinhardt, S. Roos, and H. Liebertz, Appl. Phys. Lett. **69**, 179 (1996).
[44] H. W. Sheng, W. K. Luo, F. M. Alagir, J. M. Bai, and E. Ma, Nature (London) **439**, 419 (2006).